Received: January 24, 2024. Revised: May 22, 2024. 622

International Journal of
Intelligent Engineering & Systems

http://www.inass.org/

SOM based Multi-Stage CBIR Method Using the Features of CPVTH, POPMV and MDLBP Integrated with Multi-Query

J. Anto Germin Sweeta[1]* B. Sivagami[2]

[1]*Department of Computer Science & Research Centre, S.T. Hindu College, Manonmaniam Sundaranar University, Tirunelveli, Tamil Nadu, India*
[2]*Department of Computer Science & Applications, S.T. Hindu College, Manonmaniam Sundaranar University, Tirunelveli, Tamil Nadu, India*
* Corresponding author's Email: antogerminsweeta@yahoo.com

Abstract: Content-based image retrieval (CBIR) is a significant research area focused on developing effective techniques for managing large image collections and facilitating efficient retrieval. The primary steps in CBIR involve extracting features from both query and database images and identifying database images with similar extracted features to the query image. The choice of feature extraction methods is crucial, and similarity matching is equally important. The quality of retrieval results depends on the design of the similarity matching process, as it determines how well the system matches the query image's features with those in the database, ranks highly matched database images, and presents them in the retrieval process. In this paper, an innovative content-based image retrieval framework is proposed, which is known as 'SOM based multi-stage CBIR method using the features of CPVTH, POPMV and MDLBP integrated with Multi-Query (CBIR_SCPMMQ).' By incorporating the core concepts of CPVTH, POPMV, MDLBP, and SOM, along with a multi-stage and multi-query-based retrieval system, this proposed CBIR framework offers a dynamic approach to the world of computer vision. Experimental tests on various image databases, including natural, medical, remote sensing, and texture images, have shown that CBIR_SCPMMQ outperforms the existing CBIR methods in terms of precision and retrieval accuracy. The proposed CBIR_SCPMMQ method demonstrates the improvements in precision by 9.03%, recall by 8.3%, sensitivity by 8.6%, accuracy by 2.01%, and FScore by 8.02%. Therefore, the proposed CBIR_SCPMMQ method outperforms other established CBIR techniques.

Keywords: Feature descriptor, Similarity measurement, Neural network, Self-organizing map, Multi-stage CBIR, Multi-query CBIR.

1. Introduction

Recently, content-based image retrieval has drawn a lot of interest. It retrieves the desired images from enormous databases using the features that have been extracted from both the query image and matching images found by the similarity measure algorithm. It has been discovered that texture, shape and color features, which are content-based, work well for distinguishing the relevant from irrelevant images in a system. Many cutting-edge procedures have been included into the CBIR in recent years. [2] Medical field extensively uses CBIR system for various causes such as detection, diagnosis, decision making, clinical knowledge, etc. CBIR system using various transform features is used for colonography cancer screening procedure [1]. The fusion of color, shape and texture descriptors aids the CBIR system to process the various medical image types like Computer Tomography (CT), X-ray [3], and Magnetic Resonance Imaging (MRI). The random walk model based CBIR system does image annotation effectively [4]. The Relevance Feedback (RF) is a user interaction module which allows the users to select the relevant images from the retrieval results. Implementation of CBIR based RF using feature selection model in online mode boots the retrieval performance [5]. CBIR system along with multimorbidty metric learning enhances the

pathology classification [6]. In Earth Observation (EO) field, the CBIR system using Principle Component Analysis (PCA) and clustering concept boosts the semantic categorization and region-based similarity measurement which contributes in resolving the semantic gap issue [7, 9]. The texture descriptor uses pattern to detect and extract the visual content of the image [8]. Similarity measure based on Fuzzy technique does the texture feature similarity comparison in the efficient manner [10]. The CBIR system seems to be all-rounder having solutions for all real-time image management issues. Similarity measurement plays vital role as same as feature extraction in the CBIR system. This vital combination inspires to propose a novel CBIR algorithm. The significant components of the proposed work are as per the following:

- An innovative and potential CBIR methodology named 'SOM based multi-stage CBIR method using the features of CPVTH, POPMV and MDLBP integrated with Multi-Query (CBIR_SCPMMQ)' is presented.
- Combination of three potential feature descriptors serves as the feature extraction technique in this research. The new feature matching strategy named 'Multi Stage and Multi Query based Similarity matching using SOM (MSMQS)'.
- This new CBIR_SCPMMQ algorithm solves the challenges of the existing methods in case of retrieval accuracy.

The remainder of the paper is coordinated as: Section 2 holds the related work of the CBIR domain, Section 3 depicts the proposed CBIR approach, Section 4 and 5 portray the assessment performed and its outcomes are discussed. Finally, Section 6 presents conclusion of the paper.

2. Related works

The progress in CBIR has left a lasting impression on researchers in the field of image processing which inspiring them to showcase their unique contributions. This section explores some of the CBIR methodologies that have gained widespread support in the Image Retrieval (IR) domain.

Li et al. [11] introduced a CBIR system featuring a rapid similarity feature search scheme. The experimental results lay the groundwork for a highly efficient and accurate palmprint-based personal identification system, poised for further development. The disadvantage is misidentifications or false positives in the retrieval process. Ye et al. [12] proposed the query-adaptive similarity measures and hash code-based image search techniques for Content-Based Remote Sensing Image Retrieval (CBRSIR) systems yet there is a room to improve the way of extracting and matching the features. One potential disadvantage of the proposed method for remote sensing image retrieval is its complexity and potential computational overhead. Liu et al. [13] unveiled a mobile version of CBIR that incorporates cloud computing and Deep Learning (DL) technologies with inefficient retrieval process. Disadvantage of the proposed framework is its dependency on cloud servers for image retrieval. Swati et al. [14] put forwarded a feature extraction technique based on Convolutional Neural Networks (CNN) for CBMIR systems dedicated to brain tumor research which have time complexity issue. When a model learns to memorize the training data instead of generalizing to new data, overfitting occurs. Khan, A., et al., [15] developed Directional Magnitude Local Hexadecimal Patterns (DMLHP), a unique texture descriptor that uses the texture's direction and magnitude to identify the most pertinent photos. Experiments show that the suggested DMLHP description performs far better, achieving 95% on AT&T, 92% on BT, and 99% on MIT Vistex. A drawback arises when Overfitting takes place, wherein a model focuses on memorizing the training data instead of capturing the underlying patterns. Renita et al. [16] presented a data mining-oriented grey image classification scheme for the CBMIR technology. Searching the entire database for each query image could lead to scalability issues, making it impractical for use in large-scale medical image repositories. Alshehri [17] showed that Neural Network (NN)-based CBRSIR systems contribute to better information prediction except when dealing with the hyperspectral satellite images. The effectiveness of the proposed technique may vary with the scale of the image dataset and the complexity of the retrieval tasks. Pinto et al. [18] designed a CBIR system based on Self-Organizing Maps (SOM) for thumbnail extraction purposes. The reliance on clustering algorithms for organizing the graphical data may introduce limitations in terms of scalability and adaptability to diverse datasets. Zhu et al. [19] introduced CBIR systems that harness the full potential of the network through a pooling concept with curriculum design which only uses three-stage training process. The increased complexity of the model might reduce its interpretability is its limitation. Kumar et al. [20] utilized tetrolet transformation and mid-rise quantization methods on primary features. Techniques like adaptive tetrolet transform often involve parameter tuning, which adds

another layer of complexity to the implementation. Yun et al. [21] presented the CBIR system that employ image-feature hashing to aid pairwise similarity measurement. It may exhibit reduced generalization performance and may not perform as well on diverse or real-world datasets. Mehbodniya, A., et al., [22] suggested the 'Median Binary Pattern', a combination of the multichannel decoded Local Binary Pattern (mdLBP) used for color visualization. By using Noise Robust Binary Patterns, the suggested method outperformed previous techniques, achieving Average Recovery precision (ARP) and Average Recovery rate (ARR) of 68.1 and 33.55, respectively. Limitation is increased computational complexity due to the utilization of Noise Robust Binary Patterns. Vieira, G.S., et al., [23] presented the CBIR-ANR system, which combines the accuracy noise reduction (ANR) technique with content-based image retrieval (CBIR) to modify query responses and boost assertiveness in image retrieval. Additionally, the software creates a 187-dimensional feature vector by combining three low-level features, which is competitive with prior work and size efficient for large-scale data sets. The disadvantage is inability to handle diverse image characteristics,

CBIR system development faces challenges, such as computational complexity, slow operations, limited image type support lack of scalability computational inefficiency in large-scale retrieval tasks. To overcome these, the innovative CBIR_SCPMMQ approach is explored, aiming to enhance retrieval processes, tackle drawbacks, and advance CBIR technology.

3. Proposed methodology

In this research, a new image-feature matching algorithm is introduced namely, ‘Multi Stage and Multi Query based Similarity matching using SOM (MSMQS)’. The feature set of the proposed CBIR_SCPMMQ method incorporates three different features drawn from CPVTH, POPMV, and MDLBP which yields a promising image retrieval accuracy benefited from the small quantity features which exploits a premium range of image retrieval. Fig. 1 shows the overall building blocks of the CBIR_SCPMMQ. The proposed CBIR_SCPMMQ method is subdivided into the following four modules to have a better understanding on the workflow of the algorithm, which will be discussed as follows.

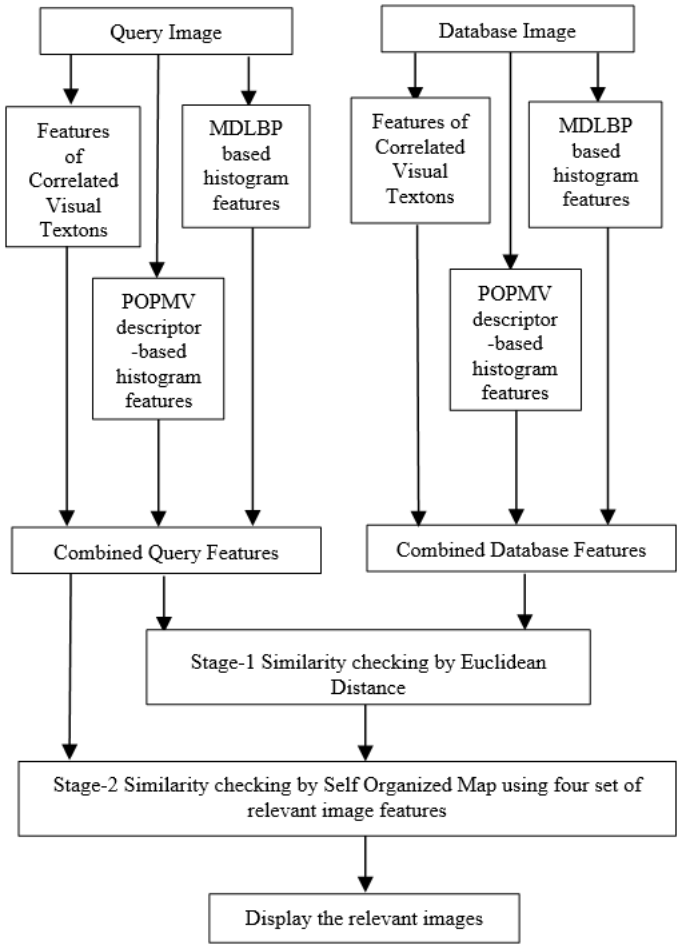

Figure. 1 Overall building blocks of the proposed CBIR_SCPMMQ method

3.1. Feature extraction based on CPVTH

The query color image I_Q which belongs to the format of '24-bit jpeg' is used as input to this method. The I_Q image is reduced to the size of 256×256 to support the reduction of time consumption. An existing feature set named 'Correlated Primary Visual Texton Histogram Features (CPVTHF)' merges semantic data with visual content through three steps: (i) generation of texture, color and intensity maps, (ii) texton images based on three maps, and (iii) co-occurrence matrix histogram features. The length of Feature quantification set for Edge information is 75, HSV color space intensity map is 40, and RGB color map is 127. The texton detection procedure generates texton images using texton templates and co-occurrence matrix-format histograms. The color map feature histogram of length 32 is noted as H_{CM}, texture orientation map histogram of length 25 is noted as H_{TOM} and intensity map histogram of length 20 is noted as H_{IM}.

3.2. Feature extraction based on POPMV

Peak-oriented Octal Pattern-derived Majority Voting (POPMV) is a feature descriptor which stores the image feature as octal-based data in 2-D matrix during the feature extraction process. When the POPMV descriptor receives an image, it converts the image color space to grey color. The foreground of the converted grey image is segmented. The segmented area serves as the neighbor element oriented 3x3 size window separation. Three highest peak indexes from both the positive and negative histograms are found. Further, the majority voting process leads to end of the descriptor process. Finally, this descriptor derives eight length histograms H_{POPMV} feature set.

3.3. Feature extraction based on MDLBP

Multichannel Decoded Local Binary Pattern (MDLBP) is a feature descriptor which maintains the co-occurrence information of the LBP cross channels using the adder and decoder. The histogram feature vector is computed for each adder and decoder. This histogram H_MDLBP set is divided by eight to quantize about 32 bins.

3.4. Image similarity measure based on MSMQS

This research proposes a new algorithm namely MSMQS to match and retrieve the relevant images based on the five histograms features from the large dataset. This innovative MSMQS algorithm retrieves relevant images using multi-stages based on content-based methods by combining five query-feature sets to construct a final query-feature vector. The main concepts set in this algorithm are: Multi stage process, Multi query-based operation, Stage I-Euclidean distance-based similarity matching, and Stage II SOM based similarity matching.

Fig. 2 shows the building blocks of the proposed MSMQS image similarity checking method. In Stage I retrieval process, the Euclidean distance method compares the similarities among the extracted features of user query and database images. In Stage II, the first seven relevant images of retrieval-set along with the user given query image are treated as next set of query images. The similarities among these extracted features are further compared using the SOM strategy combined with Euclidean distance. Finally, based on the stage II similarity comparison a set of 20 highly relevant images is retrieved which shows the efficacy of the proposed CBIR_SCPMMQ framework.

Stage I - Euclidean distance-based similarity matching

Euclidean distance is a similarity measure based on Pythagorean Theorem. Those features are utilized in an important segment of the CBIR system called 'similarity matching'. This feature extraction strategies generates a feature set which includes five histograms such as, Texture orientation map histogram H_{TOM}, Intensity map histogram H_{IM}, Color map histogram H_{CM}, POPMV descriptor histogram H_{POPMV}, MDLBP descriptor histogram H_{MDLBP}. The CBIR_SCPMMQ method produces query feature set Q_F which holds histogram features generated by the CPVTH, POPMV, and MDLBP descriptors. It is represented using Eq. (1).

$$Q_F = \left\{H_{TOM}^{i=0\ to\ 24}, H_{IM}^{i=0\ to\ 19}\right\} \quad (1)$$

where, Q_F - Query features vector. The length of the vector Q_F is 117 (i.e. $25 + 20 + 32 + 8 + 32$) which is quoted as L. The proposed CBIR_SCPMMQ method generates a feature set namely DB_F for n database-images, which holds histogram features, which is represented using Eq. (2).

$$DB_F^{k,i=0\ to\ 116} = \left\{DH_{TOM}^{i=0\ to\ 24}, DH_{IM}^{i=0\ to\ 19}\right\} \quad (2)$$
$$k \in [0, n-1]$$

where, DB_F - Database feature vector, k - Index representing the k^{th} image. The dimension of database feature vector is $n \times 117$. Herein, 117 means the length of feature vector. The Euclidean distance for k^{th} image is determined using Eq. (3).

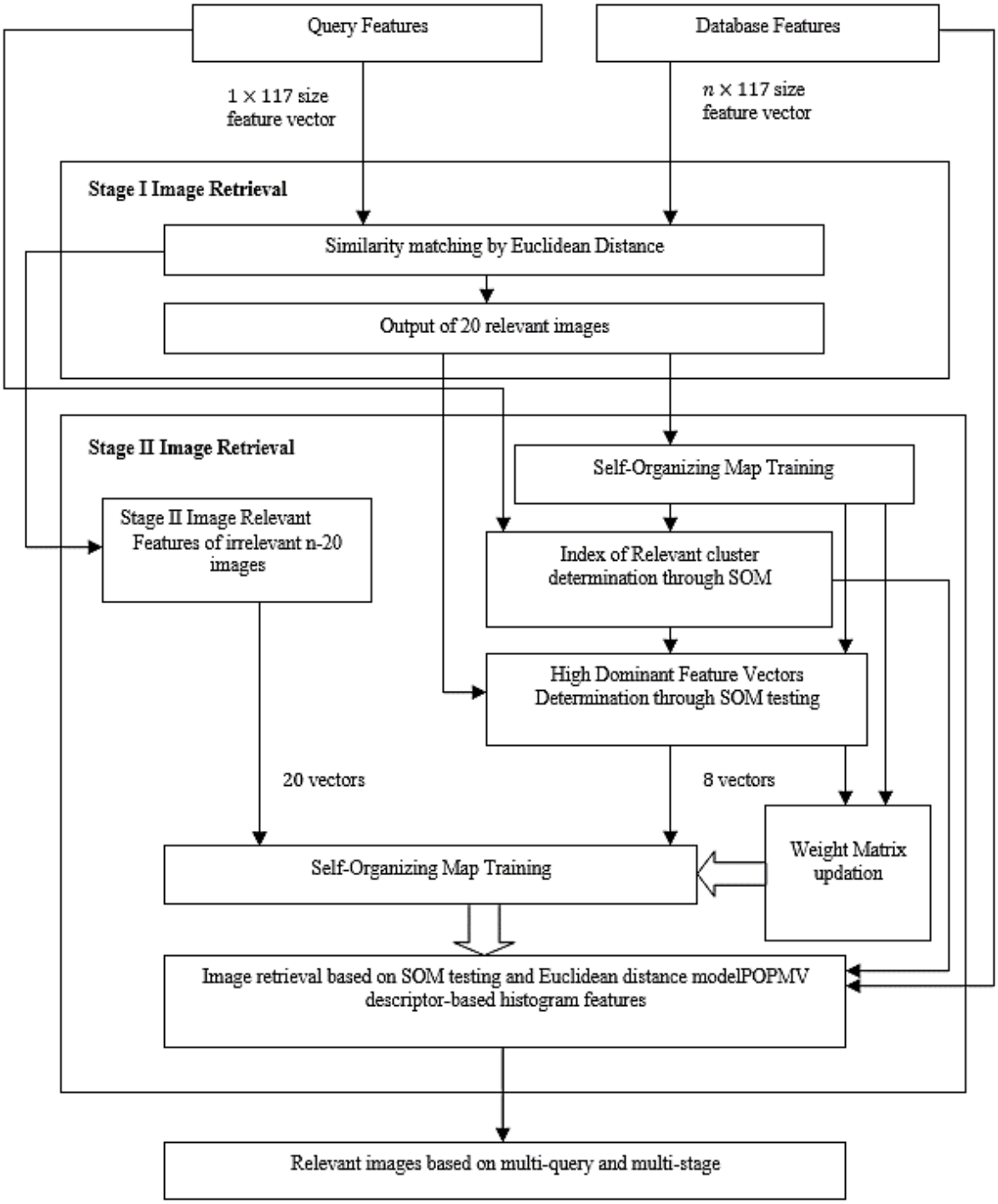

Figure. 2 Block diagram of the proposed MSMQS based similarity matching

$$\Delta^k = \sqrt{\sum_{i=0}^{116}(Q_F^i - DB_F^{k,i})^2} \qquad (3)$$
$$k \in [0, n-1]$$

where, Δ^k - Euclidean distance between query versus k^{th} image of database. The less-distance values appear in the start-up locations because the distance vector Δ is sorted in ascending order. The Stage I resultant image feature set is known as $S_1^{i,j}$, where $i \in [0,19]$ and $j \in [0, L-1]$.

Stage II-SOM based similarity matching

Self-Organizing Map (SOM) is a power-packed neural network concept coined by Teuvo Kohonen. The workflow of the stage II similarity matching is described in Fig. 2. Stage II is sub divided into the following models: Binary clustering of 20 relevant images using SOM, Determination of high dominant image features via SOM testing.

The distance computation for data and weight matrix is calculated using Eq. (4).

$$D(j) = \sum_{I=0}^{L-1}(S_1^{0,i} - w_{i,j})^2 \quad j \in [0, m-1] \tag{4}$$

Where, $D(j)$ is Distance corresponding to j^{th} cluster. The winning cluster is computed by finding the minimum distance provider in the clusters using Eq. (5).

$$WC = \begin{cases} 0, if\ D(0) < D(1) \\ 1, else \end{cases} \tag{5}$$

Where, WC - Winning cluster index. The new weights are updated for the WC cluster using Eq. (6).

$$W_{i,j}(new) = W_{i,j}(old) + (\alpha \times (S_1^{0,i} - W_{i,j}(old))) \quad i \in [L-1], j = WC \tag{6}$$

The learning rate is also updated using Eq. (7).

$$\alpha(itr+1) = 0.5(itr) \tag{7}$$

Where, itr - Current iteration number. The same process which includes the equations from Eqs. (4) to (7) is continued for the remaining feature vectors from $S_1^{1,0\ to\ L-1}$ to $S_1^{19,0\ to\ L-1}$, to obtain the fixed trained SOM network which results the updated weight matrix.

The size of weight matrix is (L, 2). The value of 2 refers the two clusters. The query feature vector is tested against the trained-SOM and it results the matched cluster index such as 0th cluster or 1st cluster. If not seven images are available, then the available matched images of IRC are noted as dominant images and the dominant images count is quoted as C_{DI}. In general, the dominant images count is modified as $C_{DI} = C_{DI} + 1$. The dominant feature vectors are noted as $F_{DI}^{i,j}$, where $i \in C_{DI}$ and $j \in [0, L-1]$. This irrelevant feature vectors are noted as F_{II}. To increase the efficiency of this second-SOM network, cluster-0 oriented matrix-column is fully replaced by the IRC related weight values of first-SOM network. The cluster-1 of the second-SOM network is kept with the initial random numbers without any change. Then the second-SOM network is trained using the selected irrelevant F_{II} and relevant F_{DI} feature vectors, which are counted by $20 + C_{DI}$. The image retrieval results for a total of 20 images are shown in Fig. 3. All of the images of dinosaurs are successfully retrieved in this case. Fig. 4 displays the results of the proposed CBIR_SCPMMQ method's image retrieval for the query medical image. The image retrieval outcome for the query remote sensing image using the proposed CBIR_SCPMMQ approach is shown in Fig. 5. Fig. 6 shows the exactly retrieved twenty 'strip' images by the utilization of the proposed CBIR_SCPMMQ technique.

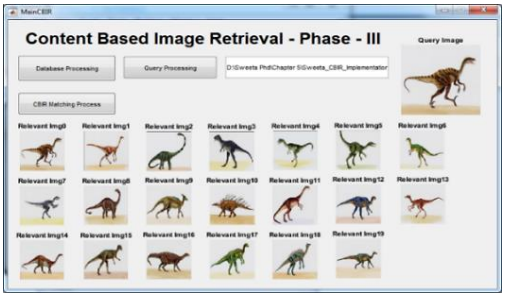

Figure. 3 Image retrieval output for query dinosaur image

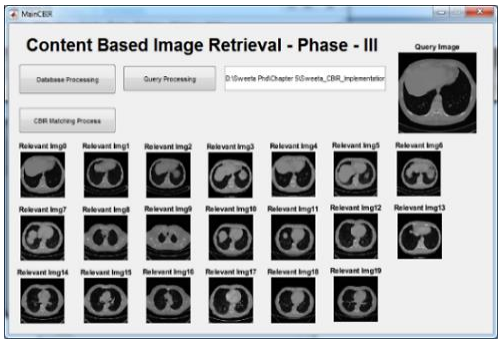

Figure. 4 Image retrieval output for query Lung image

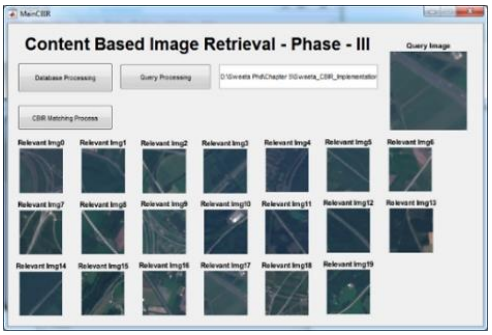

Figure. 5 Image retrieval output for query Highway table image

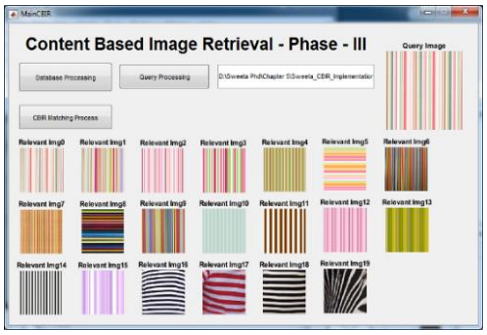

Figure. 6 Image retrieval output for query Strip image

4. Experimental results

This portion demonstrates the assessment of the performance of the CBIR_SCPMMQ system that has been suggested. The experimentation was carried out on a 64-bit Windows 10 operating system, and MATLAB application software was used for its implementation. This evaluation of proposed work encompasses four image types, and the following databases are employed such as COREL_DB [24], INDOOR_DB [25], CTMOS_DB [26], DERMO_DB [27], ESAT_DB [28], SIC_DB [29], VTEX_DB [30], and DTD_DB [31]. Here, the assessment results in Tables 1 to 3 are presented for only two image classes.

4.1. Performance evaluation

The CBIR_SCPMMQ approach is examined in comparison to four established CBIR techniques, namely CBIR_DMLPH [15], CBIR_PCS [21], CBIR_MDLBP [22], and CBIR_ANR [23]. Furthermore, the performance characteristics of CBIR_SCPMMQ are evaluated using the following parameters. Precision measures both the quantity and quality of accuracy pertaining to the given query and is calculated using Eq. (8). Where, 'w' represents the number of images in the output list retrieved and the 'OP' signifies the length of the output list.

$$Precision = w/OP \tag{8}$$

Recall, on the other hand, quantifies the number of relevant images retrieved in response to the user query from the entire database which is given in Eq. (9). Where, 'OV' represents the total count of images in the database.

$$Recall = w/OV \tag{9}$$

The sensitivity measure in the CBIR framework tracks down the value of the number of images that were correctly matched, is given in Eq. (10). Here, the False Negative (FN) demonstrates the quantity of matched images which are not correctly recognized.

$$Sensitivity = \frac{TP}{(TP+FN)} \tag{10}$$

One of the most important parameters in the image retrieval system is accuracy. Eqs. (11) and (12) are utilized to compute the specificity and accuracy of the system.

$$Specificity = \frac{TN}{(TN+FP)} \tag{11}$$

$$Accuracy = \frac{Sensitivity + Specificity}{2} \tag{12}$$

In this case, TN, FP represents True Negative and False Positive. The FScore analysis assesses the accuracy of retrieval while considering both sensitivity and specificity in balance. It is calculated using Eq. (13), where 'ab' represents the precision value and 'cd' represents the recall value.

$$FScore = (2 \times ab \times cd)/(ab + cd) \tag{13}$$

5. Discussion

Table 1 presents the precision results achieved by the CBIR_SCPMMQ method. Precision is a measure of how many retrieved instances are relevant out of all retrieved instances. The highest precision value obtained by CBIR_SCPMMQ is 0.958, indicating that it achieved very high accuracy in retrieving relevant images. Fig. 11 provides a graphical representation of precision for two image categories from each database. It visualizes the precision performance of the CBIR_SCPMMQ method. CBIR_SCPMMQ achieves the best overall results, ranging from 0.7996 to 0.9587 in precision. This suggests that the proposed method consistently outperforms other methods in terms of precision across different scenarios. CBIR_PCS method's precision values range from 0.7139 to 0.8973, indicating a lower precision compared to CBIR_SCPMMQ. CBIR_DMLPH method's precision values range from 0.6487 to 0.8529, suggesting even lower precision compared to both CBIR_SCPMMQ and CBIR_PCS. table 2 illustrates the recall assessment results of the CBIR_SCPMMQ method. Recall measures how many relevant instances were retrieved out of all relevant instances. The recall values range from 0.0046 to 0.6222, indicating the ability of CBIR_SCPMMQ to retrieve relevant images across different scenarios.

Fig. 7 highlights the sensitivity of various CBIR methods, including CBIR_MDLBP, CBIR_ANR, CBIR_DMLPH, CBIR_PCS, and the proposed CBIR_SCPMMQ. The finest accuracy results are detailed in Table 3, emphasizing the superiority of the proposed CBIR_SCPMMQ. Additionally, Fig. 12 illustrates the accuracy evaluation of two image categories from each database, where the proposed CBIR_SCPMMQ achieves a top-notch accuracy value of 88.80. Notably, CBIR_SCPMMQ consistently outperforms other methods, with accuracy ranging from 44.25 to 88.80. Comparatively, CBIR_PCS method's accuracy values range from

Table 1. Precision Evaluation of CBIR Methods

Database	Image Category	Precision				
		CBIR_ MDLBP	CBIR_ ANR	CBIR_ DMLPH	CBIR_ PCS	Proposed CBIR_SCPMMQ
COREL_DB	Bus	0.7241	0.7413	0.7939	0.8622	**0.9385**
	Beach	0.6126	0.6243	0.6487	0.7139	**0.8517**
CTMOS_DB	Lungs	0.7334	0.7619	0.7882	0.8418	**0.9228**
	Kidney	0.7257	0.7318	0.7675	0.8295	**0.9174**
ESAT_DB	Highway	0.7363	0.7423	0.7771	0.8159	**0.8943**
	Industrial	0.7548	0.7694	0.7857	0.8278	**0.9179**
VTEX_DB	Bark	0.6873	0.7148	0.7379	0.7646	**0.8188**
	Paintings	0.6593	0.6643	0.6986	0.7334	**0.7996**
INDOOR_DB	Bakery	0.6771	0.6877	0.7299	0.7548	**0.8499**
	Corridor	0.6854	0.7057	0.7576	0.8177	**0.8853**
DERMO_DB	AtypicalNevi	0.7445	0.7647	0.7833	0.8533	**0.9046**
	Melanomas	0.7792	0.8034	0.8362	0.8385	**0.8998**
SIC_DB	LandView	0.7564	0.7796	0.8045	0.8612	**0.9333**
	SeaView	0.8025	0.8338	0.8529	0.8973	**0.9587**
DTD_DB	Bubble	0.7188	0.7354	0.7618	0.8125	**0.8593**
	Fibrous	0.6959	0.7035	0.7331	0.7841	**0.8319**

Table 2. Recall Evaluation of CBIR Methods

Database	Image Category	Recall				
		CBIR_ MDLBP	CBIR_ ANR	CBIR_ DMLPH	CBIR_ PCS	Proposed CBIR_SCPMMQ
COREL_DB	Bus	0.1448	0.1482	0.1587	0.1724	**0.1877**
	Beach	0.1225	0.1248	0.1297	0.1427	**0.1703**
CTMOS_DB	Lungs	0.0037	0.0038	0.0040	0.0042	**0.0047**
	Kidney	0.0037	0.0037	0.0039	0.0042	**0.0046**
ESAT_DB	Highway	0.0058	0.0059	0.0062	0.0065	**0.0071**
	Industrial	0.0060	0.0061	0.0062	0.0066	**0.0073**
VTEX_DB	Bark	0.4582	0.4765	0.4919	0.5097	**0.5458**
	Paintings	0.4395	0.4428	0.4657	0.4889	**0.5330**
INDOOR_DB	Bakery	0.0334	0.0339	0.0360	0.0372	**0.0419**
	Corridor	0.0396	0.0407	0.0437	0.0472	**0.0511**
DERMO_DB	Atypical Nevi	0.0744	0.0764	0.0783	0.0853	**0.0904**
	Melanomas	0.0779	0.0803	0.0836	0.0838	**0.0899**
SIC_DB	LandView	0.5042	0.5197	0.5363	0.5741	**0.6222**
	SeaView	0.5177	0.5379	0.5502	0.5789	**0.6185**
DTD_DB	Bubble	0.1198	0.1225	0.1269	0.1354	**0.1432**
	Fibrous	0.1159	0.1172	0.1221	0.1306	**0.1386**

43.87 to 88.51, demonstrating its competitive performance but falling short of CBIR_SCPMMQ's consistency and peak accuracy.

Fig. 8 depicts the performance superiority of the CBIR_SCPMMQ (Content-Based Image Retrieval with Semantic Color and Pattern Matching Query) method over other selected CBIR techniques, as evaluated by the FScore metric. The FScore value, a measure of retrieval effectiveness combining precision and recall, peaks at 0.7473 for CBIR_SCPMMQ, indicating its effectiveness in retrieving relevant images. Fig. 9 showcases the average precision evaluation of CBIR methods, emphasizing retrieval performance. Notably, the proposed CBIR_SCPMMQ method achieves the highest average precision of 0.9448, signifying its ability to retrieve relevant images with high precision compared to other methods. In Fig. 10, the evaluation shifts to average accuracy assessment across CBIR methods, still focusing on retrieval performance, particularly in the VTEX_DB database. Here, CBIR_SCPMMQ again stands out, achieving the highest average accuracy of 74.07%. In contrast, CBIR_PCS and CBIR_DMLPH attain lower average accuracies of 71.84% and 70.54%, respectively. This suggests that CBIR_SCPMMQ outperforms its

Table 3. Accuracy Evaluation of CBIR Methods

Database	Image Category	Accuracy				
		CBIR_ MDLBP	CBIR_ ANR	CBIR_ DMLPH	CBIR_ PCS	Proposed CBIR_SCPMMQ
COREL_DB	Bus	52.22	52.77	53.33	53.88	**55**
	Beach	51.11	51.11	51.66	52.22	**53.88**
CTMOS_DB	Lungs	58.75	58.75	58.77	58.78	**58.80**
	Kidney	58.75	58.75	58.75	58.78	**58.80**
ESAT_DB	Highway	46.04	46.04	46.06	46.06	**46.11**
	Industrial	46.04	46.04	46.06	46.08	**46.11**
VTEX_DB	Bark	70.36	70.36	72.22	72.22	**74.07**
	Paintings	68.51	68.51	70.36	72.22	**74.07**
INDOOR_DB	Bakery	88.36	88.36	88.51	88.51	**88.80**
	Corridor	73.67	73.67	73.84	74	**74.34**
DERMO_DB	Atypical Nevi	43.12	43.12	43.50	43.87	**44.25**
	Melanomas	43.5	43.5	43.87	43.87	**44.25**
SIC_DB	LandView	52.47	55.74	55.74	59.03	**62.31**
	SeaView	49.19	49.19	52.47	55.74	**62.31**
DTD_DB	Bubble	51.84	52.31	52.31	52.77	**53.23**
	Fibrous	51.84	51.84	52.31	52.77	**53.23**

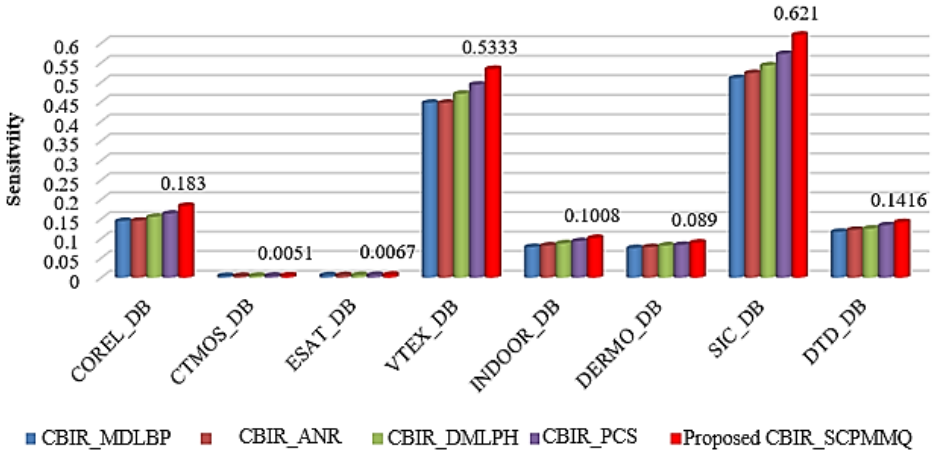

Figure. 7 Illustration of Sensitivity Assessment

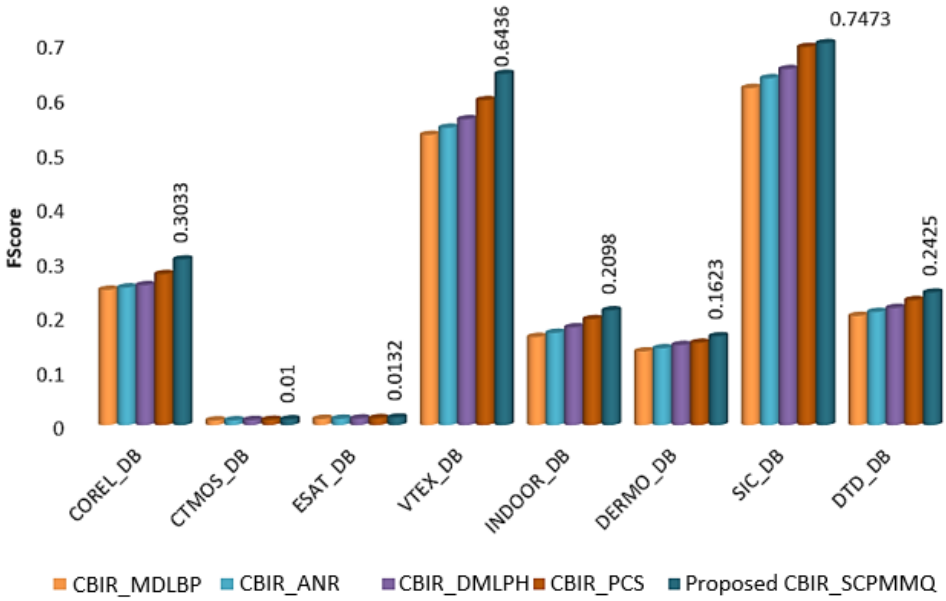

Figure. 8 Illustration of F Score Assessment

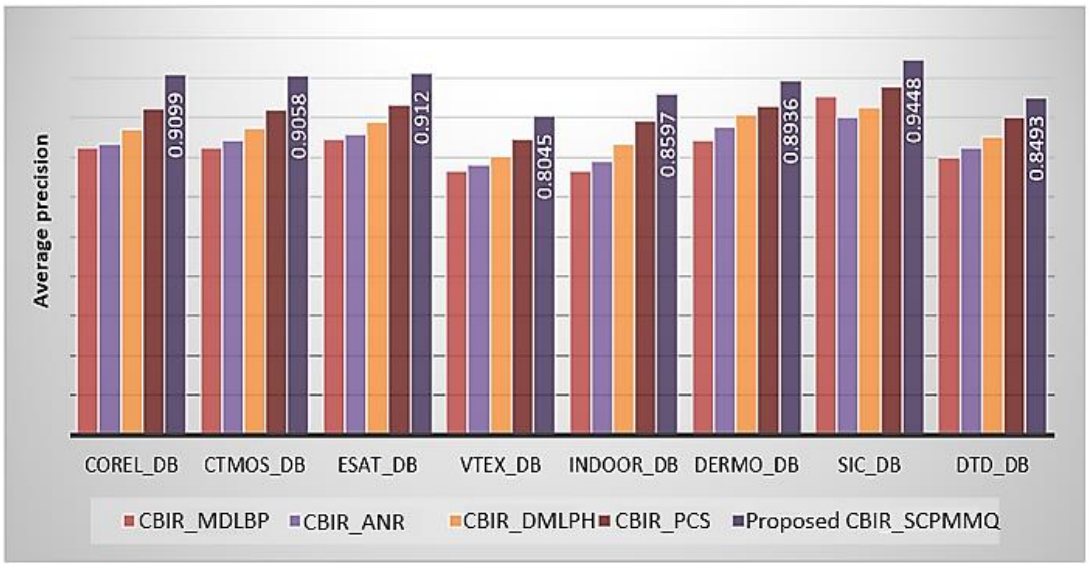

Figure. 9 Illustration of Average Precision Assessment

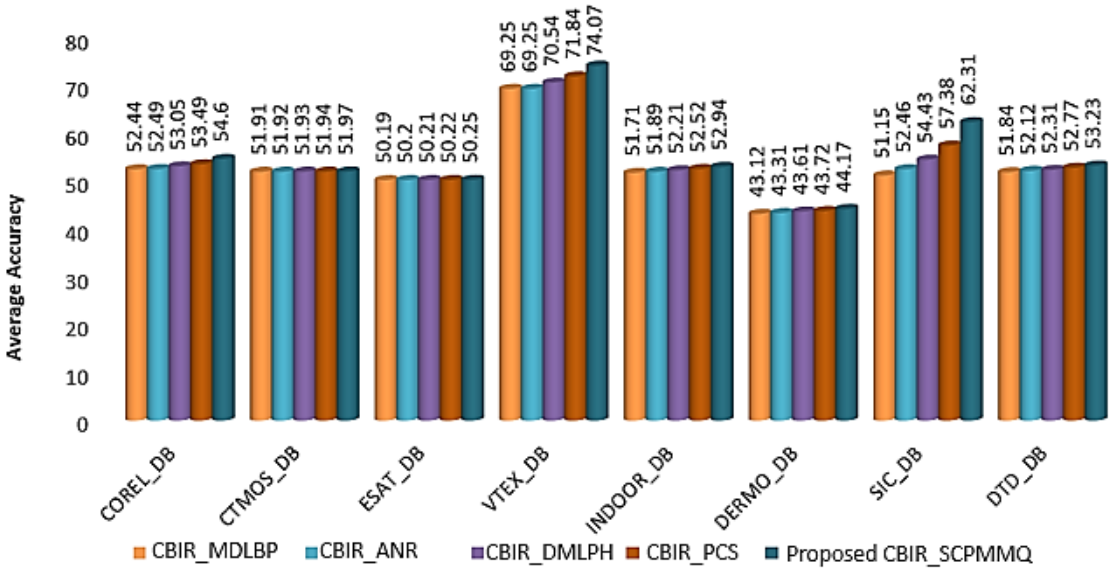

Figure. 10 Illustration of Average Accuracy Assessment

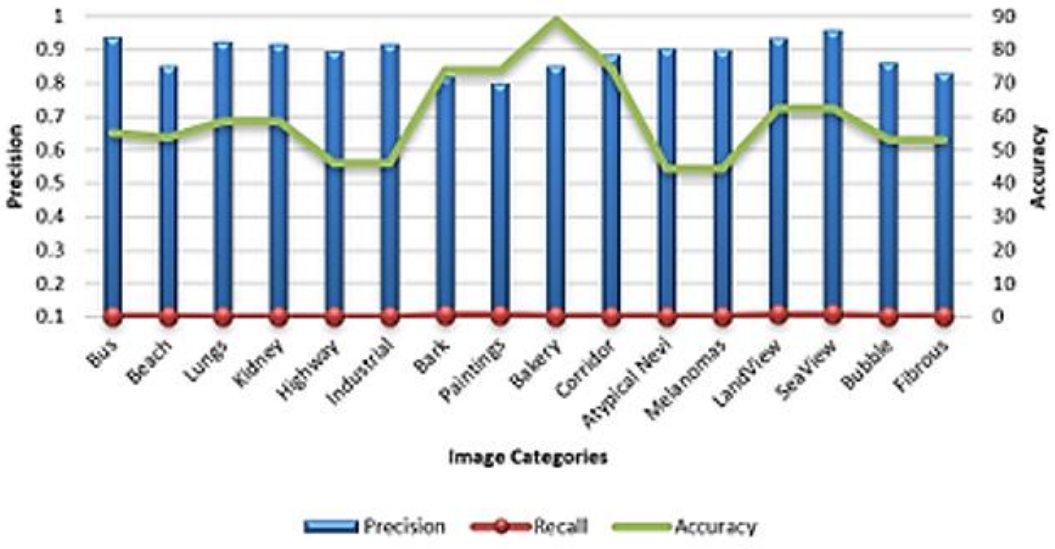

Figure. 11 Precision- Recall-Accuracy assessment outcome of the proposed CBIR_SCPMMQ method

counterparts in accurately retrieving images from the database, particularly in terms of average accuracy.

6. Conclusion

This research spotlights the importance of the innovative CBIR method known as CBIR_SCPMMQ in terms of retrieval precision, recall, and accuracy. The results from performance evaluation conducted using various metrics, clearly demonstrate the effectiveness and significance of the CBIR_SCPMMQ technique when compared to the existing methods. In comparison to the CBIR_PCS method, the proposed CBIR_SCPMMQ method demonstrates the improvements in precision by 9.03%, recall by 8.3%, sensitivity by 8.6%, accuracy by 2.01%, and FScore by 8.02%. Therefore, the proposed CBIR_SCPMMQ method outperforms other established CBIR techniques. Considering all the potential advantages of the CBIR_SCPMMQ framework, it is a valuable choice for implementation in real-time applications across various sectors. In the future, the collaboration of the proposed CBIR_SCPMMQ method with Deep Learning (DL) techniques is expected to further enhance the overall effectiveness of the CBIR framework.

Conflicts of Interest

The authors declare no conflict of interest.

Author Contributions

The following statements should be used as follows: "Conceptualization, J. Anto Germin Sweeta and B. Sivagami; methodology, J. Anto Germin Sweeta; software, B. Sivagami; validation, J. Anto Germin Sweeta, and B. Sivagami; formal analysis, B. Sivagami; investigation, J. Anto Germin Sweeta; resources, J. Anto Germin Sweeta; data curation, B. Sivagami; writing—original draft preparation, J. Anto Germin Sweeta; writing—review and editing, J. Anto Germin Sweeta; visualization, B. Sivagami; supervision, J. Anto Germin Sweeta; project administration, J. Anto Germin Sweeta; funding acquisition, B. Sivagami", etc.

Acknowledgments

The author would like to express his heartfelt gratitude to the supervisor for his guidance and unwavering support during this research for his guidance and support.

References

[1] J.M. Aman, J. Yao, and R. M. Summers, "Content-based image retrieval on CT colonography using rotation and scale invariant features and bag-of-words model", In: *Proc. of 2010 IEEE International Symposium on Biomedical Imaging: From Nano to Macro*, Vol. 1357-1360, 2010.

[2] J. Bai, X. Wang, and L. Jiao, "Image retrieval based on color features integrated with anisotropic directionality", *Journal of Systems Engineering and Electronics*, Vol. 21, No. 1, pp. 127-133, 2010.

[3] B. K. Singh, G. R. Sinha, B. Mazumdar, M. I. Khan, "Content Based Retrieval of X-ray Images Using Fusion of Spectral Texture and Shape Descriptors", In: *Proc. of 2010 International Conference on Advances in Recent Technologies in Communication and Computing*, pp. 80-84, 2010.

[4] H. Ma, J. Zhu, M.R.-T. Lyu, and I. King, "Bridging the Semantic Gap Between Image Contents and Tags", *IEEE Transactions on Multimedia*, Vol. 12, No. 5, pp. 462-473, 2010.

[5] W. Jiang, G. Er, Q. Dai, and J. Gu, "Similarity-based online feature selection in content-based image retrieval", *IEEE Transactions on Image Processing*, Vol. 15, No. 3, pp. 702-712, 2006.

[6] Y. Xing, B. J. Meyer, M. Harandi, T. Drummond, and Z. Ge, "Multimorbidity Content-Based Medical Image Retrieval and Disease Recognition Using Multi-Label Proxy Metric Learning", *IEEE Access*, Vol. 11, pp. 50165-50179, 2023.

[7] L. Jiao, X. Tang, B. Hou, and S. Wang, "SAR Images Retrieval Based on Semantic Classification and Region-Based Similarity Measure for Earth Observation", *IEEE Journal of Selected Topics in Applied Earth Observations and Remote Sensing*, Vol. 8, No. 8, pp. 3876-3891, 2015, doi:10.1109/jstars.2015.2429137

[8] A. Khan, A. Javed, M. T. Mahmood, M. H. A. Khan, and I.H. Lee, "Directional Magnitude Local Hexadecimal Patterns: A Novel Texture Feature Descriptor for Content-Based Image Retrieval", *IEEE Access*, Vol. 9, pp. 135608-135629, 2021.

[9] L. Rui, Z. Yongsheng, F. Yonghong, D. Xueqing, (n.d.). "Research on content-based remote sensing image retrieval: the strategy for visual feature selection, extraction, description and similarity measurement", In: *2001*

International Conferences on Info-Tech and Info-Net. Proceedings, pp. 321-325, 2001.

[10] P. H. Sreena, and D. S. George, "Content based image retrieval system with fuzzified texture similarity measurement", In: *Proc. of 2013 International Conference on Control Communication and Computing (ICCC)*, pp. 80-85, 2013, doi:10.1109/iccc.2013.6731628

[11] W. Li, J. You, and D. Zhang, "Texture-based palmprint retrieval using a layered search scheme for personal identification", *IEEE Transactions on Multimedia*, Vol. 7, No. 5, pp. 891-898, 2005.

[12] F. Ye, X. Zhao, W. Luo, D. Li, and W. Min, "Query-Adaptive Remote Sensing Image Retrieval Based on Image Rank Similarity and Image-to-Query Class Similarity", *IEEE Access*, Vol. 8, pp. 116824-116839, 2020.

[13] F. Liu, Y. Wang, F.-C. Wang, Y.-Z. Zhang, and J. Lin, "Intelligent and Secure Content-Based Image Retrieval for Mobile Users", *IEEE Access*, Vol. 7, pp. 119209-119222, 2019.

[14] Z. N. K. Swati, Q. Zhao, M. Kabir, F. Ali, A. Zakir, S. Ahmad, J. Lu, "Content-Based Brain Tumor Retrieval for MR Images Using Transfer Learning", *IEEE Access*, pp. 1-13, 2019.

[15] A. Khan, A. Javed, M.T. Mahmood, M. H. A. Khan, and I.H. Lee, "Directional magnitude local hexadecimal patterns: A novel texture feature descriptor for content-based image retrieval", *IEEE Access*, Vol. 9, pp. 135608-135629, 2021.

[16] D. B. Renita, and C. S. Christopher, "Novel real time content based medical image retrieval scheme with GWO-SVM", *Multimedia Tools and Applications*, pp. 1-17, 2020.

[17] M. Alshehri, "A Content-Based Image Retrieval Method Using Neural Network-Based Prediction Technique", *Arabian Journal for Science and Engineering*, Vol. 45, No. 4, pp. 2957-2973, 2019.

[18] J. Pinto, P. Jain, and T. Kumar, "A content-based image information retrieval and video thumbnail extraction framework using SOM", *Multimedia Tools and Applications*, Vol. 80, No. 11, pp. 16683-16709, 2021.

[19] X. Zhu, H. Wang, P. Liu, Z. Yang, J. Qian, "Graph-based reasoning attention pooling with curriculum design for content-based image retrieval", *Image and Vision Computing*, Vol. 115, pp. 104289, 2021.

[20] S. Kumar, J. Pradhan, A. K. Pal, "Adaptive tetrolet based color, texture and shape feature extraction for content-based image retrieval application", *Multimedia Tools and Applications*, Vol. 80, No. 19, pp. 29017-29049, 2021.

[21] H. Yun, Y. Kim, and T. Kang, K. Jung, "Pairwise context similarity for image retrieval system using variational auto-encoder", *IEEE access*, Vol. 9, pp. 34067-34077, 2021.

[22] A. Mehbodniya, J. Webber, A. G. Devi, R. P. Somineni, M. C. Chinnaiah, A. Asokan, K. S. Bhanu, "Content-Based Image Recovery System with the Aid of Median Binary Design Pattern", *Traitement du Signal*, Vol. 40, No. 2, 2023.

[23] G. S. Vieira, A. U. Fonseca, and F. Soares, "CBIR-ANR: A content-based image retrieval with accuracy noise reduction", *Software Impacts*, Vol. 15, pp. 100486, 2023.

[24] Corel-10k, 2023, Accessed from < https://www.kaggle.com/datasets/michelwilson/corel10k>, Accessed on [04-08-2023].

[25] Indoor Scene Recognition, 2009, Accessed from < https://web.mit.edu/torralba/www/indoor.html>, Accessed on [04-08-2023].

[26] CT-ORG, 2023, Accessed from < https://wiki.cancerimagingarchive.net/pages/viewpage.action?pageId=61080890>, Accessed on [04-08-2023].

[27] PH^2, 2013, Accessed from < https://www.fc.up.pt/addi/ph2%20database.html>, Accessed on [04-08-2023].

[28] Euro Sat, 2021, Accessed from < https://www.kaggle.com/datasets/saipavansaketh/eurosatland>, Accessed on [04-08-2023].

[29] SIC Database, 2014, Available from < https://www.satimagingcorp.com/gallery/>, Accessed on [19 June 2022].

[30] Vision Texture, 2002, Accessed from < https://vismod.media.mit.edu/vismod/imagery/VisionTexture/vistex.html>, Accessed on [04-08-2023].

[31] DTD Database, 2014, Available from < https://www.robots.ox.ac.uk/~vgg/data/dtd/>, Accessed on [19 June 2022].